Please do not adjust margins

ChemComm

COMMUNICATION

# hIAPP forms toxic oligomers in plasma

Diana C. Rodriguez Camargo,[a,b,c,d,*] Divita Garg,[c,d] Katalin Buday,[e] Andras Franko,[f,g] Andres Rodriguez Camargo,[h] Fabian Schmidt,[d] Sarah Cox,[b] Saba Suladze,[d] Martin Haslbeck,[d] Yonatan G. Mideksa,[a,c] Gerd Gemmecker,[d] Michaela Aichler,[i] Gabriele Mettenleiter,[i] Michael Schulz,[f,g] Axel Karl Walch,[i] Martin Hrabě de Angelis,[f,g] Matthias Feige,[a,c] Cesar A. Sierra,[h] Marcus Conrad,[e] Konstantinos Tripsianes,[j] Ayyalusamy Ramamoorthy,[a,b] Bernd Reif[a,c,d]

Received 00th January 20xx,
Accepted 00th January 20xx

DOI: 10.1039/x0xx00000x

www.rsc.org/

**In diabetes, hyperamylinemia contributes to cardiac dysfunction. The interplay between hIAPP, blood glucose and other plasma components is, however, not understood. We show that glucose and LDL interact with hIAPP, resulting in β-sheet rich oligomers with increased β-cell toxicity and hemolytic activity, providing mechanistic insights for a direct link between diabetes and cardiovascular diseases.**

Diabetes is a widespread disease affecting more than 415 million people and claiming more than 5 million lives worldwide only in 2015.[1] Type 2 diabetes (T2D) is the most common form of the disease and accounts for approximately 90% of all cases.[2] While the exact cellular pathomechanism of T2D remains elusive, at least six principal factors have been identify to contribute to T2D, which include insulin resistance, lipotoxicity, endoplasmic reticulum oxidative stress, tissue inflammation response, amyloid deposition and β-cell failure.[3, 4] Pancreatic amyloid deposits are composed of the 37 residue peptide hormone human Islet Amyloid Polypeptide (hIAPP).[5, 6] hIAPP is thought to be involved in the slowdown of post-meal increase of plasma glucose concentration.[7] The mechanism of its cytotoxicity in T2D is, however, only partially understood.[8] Recent studies have shown that soluble oligomers of hIAPP are responsible for cell toxicity and cell death.[9-11] There is only little knowledge about the factors that lead to hIAPP aggregation *in vivo*. hIAPP is stored in a functional and soluble form in insulin granules in β-cells at concentrations up to 1-4 mM.[12] The cellular environment has thus a strong impact on the rate of hIAPP aggregation. Factors affecting aggregation include pH,[13] divalent cations such as $Zn^{2+}$,[14] insulin,[15, 16] and the redox environment.[17, 18] It is known that the serum of diabetic patients contains low concentrations of high-density lipoproteins (HDL) and high concentrations of very low-density lipoproteins (VLDL), low-density lipoproteins (LDL) and plasma triglycerides (TG).[19] In addition, the concentration of sugars and insulin is increased. Whereas the blood glucose concentration in healthy individuals is on the order of 6 mM, it ranges between 10 mM and >14 mM in people affected by T2D.[20] T2D is linked with other diseases such as Alzheimer's disease,[21, 22] cardiac dysfunction in obesity,[23] kidney disease and other renal failures.[24] The aim of this study is to investigate the impact of major plasma components known to be disturbed in T2D on the kinetic and structural aspects of hIAPP oligomerization and fiber formation. We find that LDL stabilizes high molecular weight hIAPP species and effects hIAPP aggregation. We observe further that sugars induce liquid-liquid phase separation and yield increased cellular toxicity. We propose that these oligomers may be the link between T2D and associated complications such as cardiac dysfunction in obesity.

In the past, we have studied the aggregation behaviour of hIAPP *in vitro*.[18] We now want to understand how hIAPP behaves under physiological conditions. To address this question, we employ blood plasma of diabetic transgenic mice. The mouse models harbor either one (+/TG mice) or two copies (TG/TG mice) of human IAPP.[25] As a control, we used plasma of +/+ wild type mice. Although pancreatic amyloid fibrils are present in both the +/TG and TG/TG mice, only TG/TG mice are affected by diabetes.[26] It is known that the plasma of diabetic patients becomes lactescent due to an increase of dispersed lipids[27] (increasing lactescence +/+ < +/TG < TG/TG) (Fig. 1A). In addition, previous results showed decreased HDL-cholesterol

[a] *Institute for Advanced Study, Technische Universität München, 85748 Garching, Germany*
[b] *Program in Biophysics, Department of Chemistry, University of Michigan, Ann Arbor, MI, 48109-1055, USA*
[c] *Munich Center for Integrated Protein Science (CIPS-M) at Department of Chemistry, Technische Universität München, 85747 Garching, Germany*
[d] *Helmholtz Zentrum München, Institute of Structural Biology (STB), Ingolstädter Landstr. 1, 85764 Neuherberg, Germany*
[e] *Helmholtz Zentrum München, Institute of Developmental Genetics (IDG), Ingolstädter Landstr. 1, 85764 Neuherberg, Germany*
[f] *Helmholtz Zentrum München, Institute of Experimental Genetics (IEG), Ingolstädter Landstr. 1, 85764 Neuherberg, Germany*
[g] *German Center for Diabetes Research (DZD e.V.), 85764 Neuherberg, Germany*
[h] *Departament of Chemistry, Universidad Nacional de Colombia, Carrera 30 # 45-03 (Ciudad Universitaria), 111321 Bogota, Colombia*
[i] *Helmholtz Zentrum München, Research Unit Analytical Pathology (AAP), Ingolstädter Landstr. 1, 85764 Neuherberg, Germany*
[j] *Central European Institute of Technology (CEITEC), Masaryk University, Kamenice 5, 62500 Brno, Czech Republic*
*Electronic Supplementary Information (ESI) available.*



Please do not adjust margins

Please do not adjust margins



and insulin levels and high levels of plasma glucose, urea and LDL-cholesterol in hIAPP transgenic mice.[26]

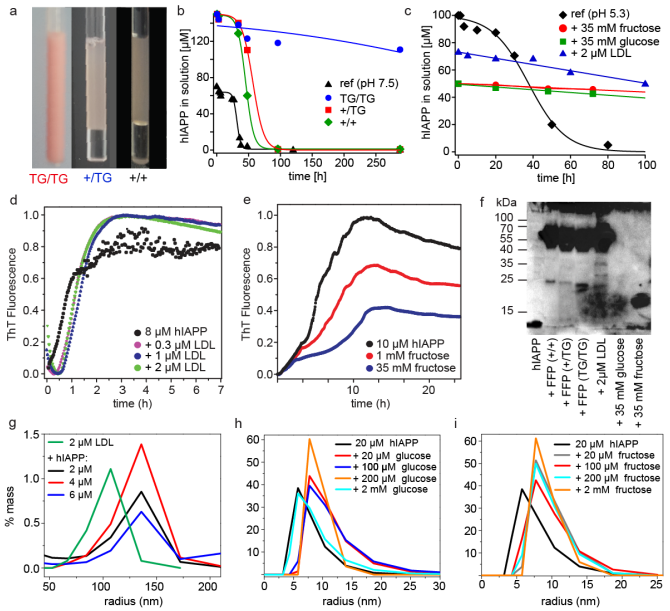


***Fig. 1. Plasma induces retardation of hIAPP aggregation and induces formation of oligomers.*** ***a*** *Plasma of +/+, +/TG and TG/TG mice. NMR hIAPP aggregation kinetics of hIAPP in* ***b*** *+/+, +/TG and TG/TG plasma, and* ***c*** *in the presence of LDL (green), fructose (grey), glucose (red). hIAPP (pH 7.5) is shown as a reference (blue). Thioflavin T (ThT) aggregation kinetics after incubation of hIAPP with* ***d*** *LDL and* ***e*** *fructose.* ***f*** *Immunoblot analysis of hIAPP oligomers in fresh frozen plasma (FFP), LDL and fructose.* ***g-i*** *Dynamic light scattering (DLS) of hIAPP complexes in the presence of LDL, glucose and fructose.*

To understand the impact of plasma composition on the conformation and behavior of hIAPP, we dissolved isotopically labeled hIAPP in plasma. As a control, the peptide was measured in a standard buffer at pH 7.5. To estimate the stability of hIAPP in solution, we followed the kinetics by monitoring the solution-state NMR signal intensities over time. We find that hIAPP is most stable in plasma of TG/TG animals (Fig. 1B). In general, the NMR signal intensities decrease more slowly if the peptide is dissolved in plasma than in reference buffer, in agreement with previous studies which showed that crowding agents can induce a retardation of aggregation.[28] Diabetic (TG/TG) and non-diabetic (+/+, +/TG) plasma differs mostly in the concentration of LDL and sugars.[29] We therefore analyzed the effect of these two components on the aggregation kinetics, as well as on the conformation of hIAPP. Aggregation of hIAPP was monitored by NMR. As illustrated in Fig. 1C, LDL and sugar solutions (fructose or glucose) had a similar stabilizing effect as TG/TG plasma. To obtain a better understanding of the aggregation kinetics, we performed Thioflavin T (ThT) assays (Fig. 1D,E). In presence of LDL, we observe an increase of the lag time. The maximum fluorescence intensity is, however, unchanged. By contrast for fructose, the maximum fluorescence is significantly reduced. The results suggest that LDL, glucose and fructose have a direct impact on the aggregation state of hIAPP. This is in agreement with results from Kedia et al. who showed that sugars favor Aβ42 oligomer formation.[30] To characterize the oligomerization state in more detail, we performed Dynamic Light Scattering (DLS) experiments. DLS reveals an increase of the hydrodynamic size of the hIAPP assemblies formed in the presence of LDL, glucose and fructose (Fig. 1G-I). In addition, we performed Western blot experiments using the hIAPP specific antibody A133 (Fig. 1F).[31] As shown previously,[18,32] hIAPP yields bands in the molecular weight range from 15 kDa to approximately 100 kDa. We find that +/+, +/TG, and TG/TG plasma induced oligomers have a similar molecular weight as the oligomers that are formed in the presence of 2 µM LDL. By contrast, glucose or fructose induced oligomers yield a band corresponding to a molecular weight on the order of 15 kDa, suggesting that hIAPP interacts differently with sugars and LDL.

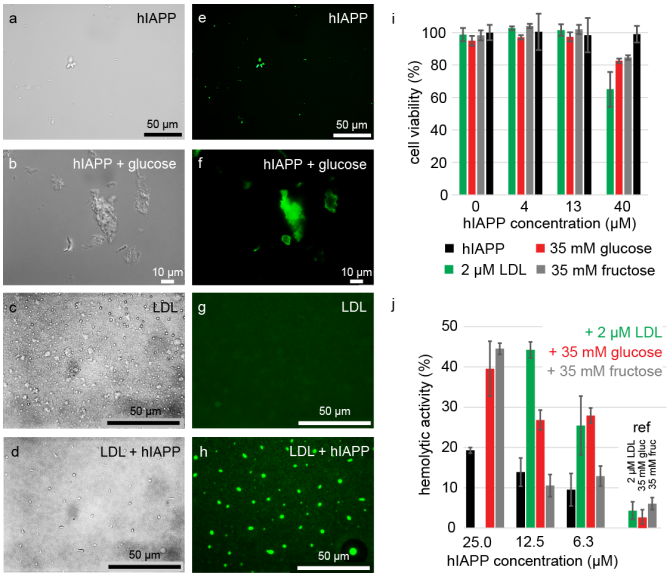


***Fig. 2. Glucose and LDL induced hIAPP yield intrinsically fluorescent oligomers with increased neurotoxicity.*** ***(a-d)*** *DIC and* ***(e-h)*** *GFP-filtered fluorescence microscopy images of hIAPP in the absence and presence of glucose and LDL.* ***i*** *b-tc3 cellular toxicity of hIAPP in the presence of 2 µM LDL, 35 mM glucose and 35 mM fructose.* ***j*** *Hemolytic activity of hIAPP in the absence (black) and presence of 2 µM LDL (green), 35 mM glucose (red) and 35 mM fructose (gray).*

To test the hypothesis whether LDL, glucose and fructose are able to induce hIAPP oligomeric structures, we carried out fluorescence and Differential Interference Contrast (DIC) microscopy experiments. We find that sugar and LDL induced hIAPP aggregates yield an intrinsic fluorescence (Fig. 2), which has been observed previously for amyloid fibrils (Fig. S3).[33,34] hIAPP alone yields only few colloidal structures. In the presence of sugars, however, larger and more aggregate structures are observed. In DIC experiments, LDL particles appear spherical and non-fluorescent. In the presence of hIAPP, however, LDL particles show an intrinsic fluorescence indicating that LDL interacts with hIAPP. To find out if these soluble oligomers are toxic *in vivo*, we carried out cellular toxicity assays using the pancreatic β-cell line b-tc3. B-tc3 cells were incubated with hIAPP in combination with glucose, LDL or fructose. Increasing concentrations of hIAPP yield a decrease of cellular viability in all cases (Fig. 2I), suggesting that LDL and glucose/fructose increase cellular toxicity. In addition, we performed a hemolytic assay to investigate whether hIAPP is able to lyse red blood cells (Fig. 2J). We find that the



This journal is © The Royal Society of Chemistry 20xx

Please do not adjust margins

Please do not adjust margins



presence of LDL or sugars such as glucose or fructose increases the hemolytic activity strongly.

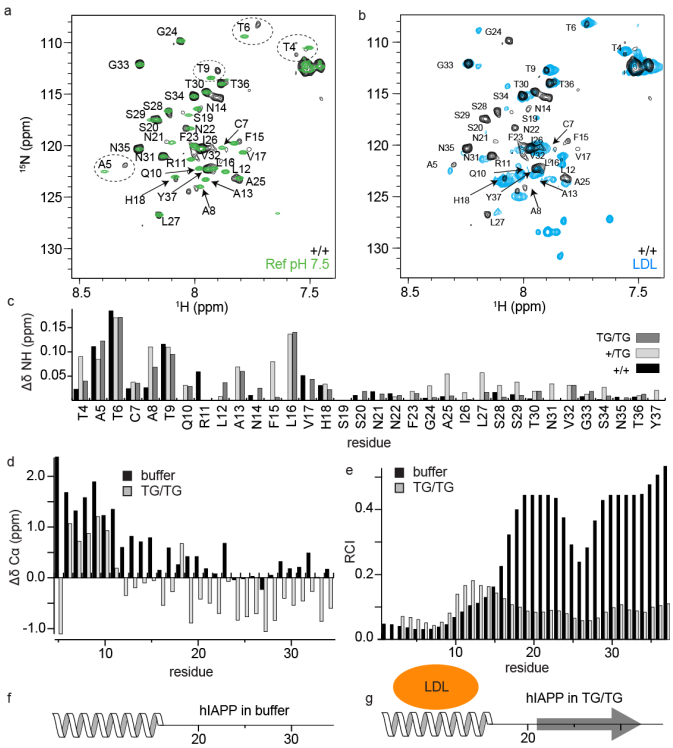


***Fig. 3. NMR analysis of hIAPP dissolved in plasma and LDL. a*** *Superposition of $^{1}$H,$^{15}$N-HMQC spectra of 100 µM hIAPP in +/+ plasma and buffer (pH 7.5) and* ***b*** *+/+ plasma and LDL.* ***c*** *Residue specific amide chemical shift differences.* ***d*** *Δδ(Cα) chemical shift differences between hIAPP in buffer (pH 7.5) and hIAPP in plasma.* ***e*** *Random Coil Index (RCI) obtained from the backbone chemical shifts for hIAPP dissolved in buffer and for hIAPP dissolved in TG/TG plasma.* ***f, g*** *Secondary structural model of hIAPP in buffer and in TG/TG plasma, respectively.*

To obtain deeper insight into the interaction mechanism, we carried out solution-state NMR experiments. First, we dissolved isotopically labeled hIAPP[35] in plasma (+/+, +/TG and TG/TG) and recorded HMQC experiments (Fig. 3A). As a control, spectra of hIAPP dissolved into phosphate buffer (pH 7.5) are recorded. Fig. 3C represents the chemical shift changes observed for the three different plasma samples with respect to the control sample. We find that chemical shifts of residues located in the N-terminal region of hIAPP are perturbed. To identify the molecules that are responsible for these shift changes, we recorded experiments for hIAPP dissolved in a 2 µM LDL solution (Fig. 3B). Many of the chemical shift changes in the N-terminal region of hIAPP observed in plasma are also seen in the presence of LDL, suggesting that lipid containing particles are responsible for these spectral changes. This observation is consistent with a previous study where it was shown that the N-terminal part of hIAPP interacts with membrane nanodiscs.[36] To characterize the structural changes in hIAPP which are induced by TG/TG plasma, we performed 3D HNCA-experiments. The analysis of the hIAPP Δδ($^{13}$Cα) chemical shift differences (Fig. 3D) suggests that the peptide is converted from a random coil structure with an α-helical propensity in phosphate buffer[18] to a conformer which is rich in β-sheet structure. The Random Coil Index (RCI) supports this finding (Fig. 3E). Based on the Δδ($^{13}$Cα) data and the RCI, we propose a secondary structure model for hIAPP in buffer and TG/TG plasma (Fig. 3F,G).

After intake of food, the blood glucose level rises, stimulating the pancreatic secretion of insulin and hIAPP. In diabetes, these two peptide hormones become overexpressed, which can drive aggregation and in turn cellular toxicity.[10] So far, aggregation of hIAPP has been observed to occur only in pancreatic beta-cells, without affecting significantly other organs. We find that key molecules in plasma which are known to be elevated in T2D, such as LDL and glucose induce a stabilization of a non-aggregation prone state of the peptide. hIAPP solubilized in plasma and LDL yields high molecular weight oligomer complexes with an apparent molecular weight in the range of ~15 kDa to ≥ 100 kDa. LDL and sugar induced hIAPP oligomers yield an increased hemolytic activity as well as cellular toxicity. Interestingly, the LDL/sugar induced hIAPP oligomeric assemblies display an intrinsic fluorescence. This might indicate that β-sheets are already preformed in these oligomeric structures, as otherwise no intrinsic fluorescence would be observed. Intrinsic fluorescence of oligomeric Aβ assemblies has been observed previously by super-resolution microscopy.[37] By NMR, we have observed that the peaks originating from residues located in the N-terminal region of the peptide are changing in chemical shift in the presence of diabetic plasma and LDL, suggesting that this part of hIAPP is involved in interactions with the respective plasma components. At the same time, the C-terminal part of the peptide adopts a certain propensity for β-sheet structure. For the hIAPP - glucose/fructose mixtures, no chemical shift changes are observed after mixing. We find, however, that aggregation of hIAPP is significantly retarded in the presence of sugars. Under these conditions, hIAPP populates oligomers that yield a reduced ThT fluorescence signal, but a very pronounced intrinsic fluorescence. In EM, hIAPP adopts very thin and fragile protofibrillar structures in presence of fructose and glucose (Fig. S2). We speculate that sugars might induce formation of hIAPP-rich colloidal structures. In fact, glucose is a cosmotropic osmolyte,[38,39] coordinates water and gets excluded from interactions with the hIAPP backbone, thereby inducing structure. At the same time, hIAPP might exchange between a high molecular weight and a monomeric state which would allow to explain the relatively high intensities observed in the NMR experiments. In case of LDL, EM shows that hIAPP aggregates are lined up along a series of LDL particles (Fig. S2). The presence of a lipid particle might catalyze the transition between a monomeric and a high molecular weight state of hIAPP, which might facilitate the detecton of a hIAPP monomeric state. The plasma concentration of hIAPP has been reported to be in the pM range.[40, 41] Nevertheless, antibodies which specifically recognize oligomeric hIAPP assemblies were identified in the serum of diabetic patients,[10] suggesting that hIAPP oligomers can assemble even at these very low concentrations.

In conclusion, we have shown that hIAPP, LDL, and sugars mutually interact, suggesting a direct link between TD2 and cardiovascular diseases.



Please do not adjust margins

Please do not adjust margins



This work was performed in the framework of the SFB-1035 (project B07 and -B11, Deutsche Forschungsgemeinschaft, DFG, to B.R. and M.J.F.). We acknowledge support from the Technische Universitaet Muenchen, Institute for Advanced Study (IAS), funded by the German Excellence Initiative and the European Union Seventh Framework Program, grant no. 291763. M.J.F. is an IAS Rudolf Mößbauer Tenure Track Professor. A.R. is supported by an IAS Hans Fischer Senior Fellowship. Y.M. and M.J.F. gratefully acknowledge funding by a DAAD PhD scholarship. A.R. was partly supported by funds from NIH (AG048934). K.T. acknowledges support from the MEYS of the Czech Republic under the project CEITEC 2020 (LQ1601). We are grateful to Gunilla Westermark for providing us with a sample of the antibody A133. Furthermore, we would like to thank Dr. Christoph Goebl, Dr. Vanessa Morris, Dr. Sam Asami and Dr. Carina Motz for stimulating discussions.

## Notes and references

1. K. Ogurtsova, J. da Rocha Fernandes, Y. Huang, U. Linnenkamp, L. Guariguata, N. Cho, D. Cavan, J. Shaw and L. Makaroff, Diabetes Res. Clin. Pract., 2017, 128, 40-50.
2. T. Scully, Nature, 2012, 492, S2-S3.
3. A. F. Amos, D. J. McCarty and P. Zimmet, Diabetic Med., 1997, 14 Suppl 5, S1-S85.
4. M. Y. Donath and S. E. Shoelson, Nature Rev. Immunol., 2011, 11, 98-107.
5. P. Westermark, C. Wernstedt, E. Wilander, D. W. Hayden, T. D. Obrien and K. H. Johnson, Proc. Natl Acad. Sci. U.S.A., 1987, 84, 3881-3885.
6. G. J. S. Cooper, A. C. Willis, A. Clark, R. C. Turner, R. B. Sim and K. B. M. Reid, Proc. Natl Acad. Sci. U.S.A., 1987, 84, 8628-8632.
7. A. J. Percy, D. A. Trainor, J. Rittenhouse, J. Phelps and J. E. Koda, Clin. Chem., 1996, 42, 576-585.
8. P. Cao, P. Marek, H. Noor, V. Patsalo, L. H. Tu, H. Wang, A. Abedini and D. P. Raleigh, FEBS Lett., 2013, 587, 1106-1118.
9. C. Y. Lin, T. Gurlo, R. Kayed, A. E. Butler, L. Haataja, C. G. Glabe and P. C. Butler, Diabetes, 2007, 56, 1324-1332.
10. Y. Bram, A. Frydman-Marom, I. Yanai, S. Gilead, R. Shaltiel-Karyo, N. Amdursky and E. Gazit, Sci. Rep., 2014, 4, 04267.
11. A. Abedini, A. Plesner, P. Cao, Z. Ridgway, J. H. Zhang, L. H. Tu, C. T. Middleton, B. Chao, D. J. Sartori, F. L. Meng, H. Wang, A. G. Wong, M. T. Zanni, C. B. Verchere, D. P. Raleigh and A. M. Schmidt, Elife, 2016, 5.
12. J. C. Hutton, Diabetologia, 1989, 32, 271-281.
13. L. Khemtémourian, E. Doménech, J. P. Doux, M. C. Koorengevel and J. A. Killian, J. Am. Chem. Soc., 2011, 133, 15598-15604.
14. J. R. Brender, K. Hartman, R. P. R. Nanga, N. Popovych, R. D. Bea, S. Vivekanandan, E. N. G. Marsh and A. Ramamoorthy, J. Am. Chem. Soc., 2010, 132, 8973-8983.
15. J. L. Larson and A. D. Miranker, J. Mol. Biol., 2004, 335, 221-231.
16. L. Wei, P. Jiang, Y. H. Yau, H. Summer, S. G. Shochat, Y. G. Mu and K. Pervushin, Biochemistry, 2009, 48, 2368-2376.
17. B. W. Koo and A. D. Miranker, Prot. Sci., 2005, 14, 231-239.
18. D. C. Rodriguez Camargo, K. Tripsianes, K. Buday, A. Franko, C. Göbl, C. Hartlmüller, R. Sarkar, M. Aichler, G. Mettenleiter, M. Schulz, A. Böddrich, C. Erck, H. Martens, A. K. Walch, T. Madl, E. E. Wanker, M. Conrad, M. Hrabě de Angelis and B. Reif, Sci. Rep., 2017, 7, 44041.
19. M. Guérin, W. Le Goff, T. S. Lassel, A. Van Tol, G. Steiner and M. J. Chapman, Arterioscler. Thromb. Vasc. Biol., 2001, 21, 282-288.
20. J. W. van Dijk and L. J. van Loon, Diabetes Spectr., 2015, 28, 24-31.
21. C. L. Leibson, W. A. Rocca, V. A. Hanson, R. Cha, E. Kokmen, P. C. Obrien and P. J. Palumbo, Am. J. Epidemiol., 1997, 145, 301-308.
22. A. Ott, R. P. Stolk, F. van Harskamp, H. A. P. Pols, A. Hofman and M. M. B. Breteler, Neurology, 1999, 53, 1937-1942.
23. S. Boudina and E. D. Abel, Circulation, 2007, 115, 3213-3223.
24. W. Gong, Z. Liu, C. Zeng, A. Peng, H. Chen, H. Zhou and L. Li, Kidney Int., 2007, 72, 213-218.
25. C. B. Verchere, D. A. Dalessio, R. D. Palmiter, G. C. Weir, S. BonnerWeir, D. G. Baskin and S. E. Kahn, Proc. Natl Acad. Sci. U.S.A., 1996, 93, 3492-3496.
26. A. Franko, D. C. Rodriguez Camargo, A. Böddrich, D. Garg, A. Rodriguez Camargo, J. Rozman, B. Rathkolb, D. Janik, M. Aichler, A. Feuchtinger, F. Neff, H. Fuchs, E. E. Wanker, B. Reif, H.-U. Häring, A. Peter and M. Hrabě de Angelis, Sci. Rep., 2018, 8, article no. 1116.
27. K. Tremblay, J. Methot, D. Brisson and D. Gaudet, J. Clin. Lipid., 2011, 5, 37-44.
28. J. Seeliger, A. Werkmuller and R. Winter, Plos One, 2013, 8.
29. A. Franko, S. Neschen, J. Rozman, B. Rathkolb, M. Aichler, A. Feuchtinger, L. Brachthauser, F. Neff, M. Kovarova, E. Wolf, H. Fuchs, H. U. Haring, A. Peter and M. H. de Angelis, Mol. Metabol., 2017, 6, 256-266.
30. N. Kedia, M. Almisry and J. Bieschke, Phys. Chem. Chem. Phys., 2017, 19, 18036-18046.
31. J. F. Paulsson and G. T. Westermark, Diabetes, 2005, 54, 2117-2125.
32. M. E. Oskarsson, J. F. Paulsson, S. W. Schultz, M. Ingelsson, P. Westermark and G. T. Westermark, Am. J. Pathol., 2015, 185, 834-846.
33. F. T. S. Chan, G. S. K. Schierle, J. R. Kumita, C. W. Bertoncini, C. M. Dobson and C. F. Kaminski, Analyst, 2013, 138, 2156-2162.
34. L. L. del Mercato, P. P. Pompa, G. Maruccio, A. Della Torre, S. Sabella, A. M. Tamburro, R. Cingolani and R. Rinaldi, Proc. Natl Acad. Sci. U.S.A., 2007, 104, 18019-18024.
35. D. C. Rodriguez Camargo, K. Tripsianes, T. G. Kapp, J. Mendes, J. Schubert, B. Cordes and B. Reif, Protein Expr. Purif., 2015, 106, 49–56.
36. D. C. Rodriguez Camargo, K. J. Korshavn, A. Jussupow, K. Raltchev, D. Goricanec, M. Fleisch, R. Sarkar, K. Xue, M. Aichler, G. Mettenleiter, A. K. Walch, C. Camilloni, F. Hagn, B. Reif and A. Ramamoorthy, eLife, 2017, 6, e31226.
37. G. S. K. Schierle, S. van de Linde, M. Erdelyi, E. K. Esbjorner, T. Klein, E. Rees, C. W. Bertoncini, C. M. Dobson, M. Sauer and C. F. Kaminski, J. Am. Chem. Soc., 2011, 133, 12902-12905.
38. T. O. Street, D. W. Bolen and G. D. Rose, Proc. Natl. Acad. Sci. USA, 2006, 103, 13997-14002
39. M. B. Burg and J. D. Ferraris, J. Biol. Chem., 2008, 283, 7309-7313.
40. P. C. Butler, J. Chou, W. B. Carter, Y. N. Wang, B. H. Bu, D. Chang, J. K. Chang and R. A. Rizza, Diabetes, 1990, 39, 752-756.
41. R. A. Pittner, K. Albrandt, K. Beaumont, L. S. L. Gaeta, J. E. Koda, C. X. Moore, J. Rittenhouse and T. J. Rink, J. Cell. Biochem., 1994, 55, 19-28.

 This journal is © The Royal Society of Chemistry 20xx

Please do not adjust margins

**Supporting Information**
**for the manuscript**

# hIAPP forms toxic oligomers in plasma

Diana C. Rodriguez Camargo,[a,b,c,d,*] Divita Garg,[c,d] Katalin Buday,[e] Andras Franko,[f,g] Andres Rodriguez Camargo,[h] Fabian Schmidt,[d] Sarah Cox,[b] Saba Suladze,[d] Martin Haslbeck,[d] Yonatan G. Mideksa,[a,c] Gerd Gemmecker,[d] Michaela Aichler,[i] Gabriele Mettenleiter,[i] Michael Schulz,[f,g] Axel Karl Walch,[i] Martin Hrabě de Angelis,[f,g] Matthias Feige,[a,c] Cesar A. Sierra,[h] Marcus Conrad,[e] Konstantinos Tripsianes,[j] Ayyalusamy Ramamoorthy,[a,b] Bernd Reif[a,c,d]

April 27, 2018

*a Institute for Advanced Study, Technische Universität München, 85748 Garching, Germany*
*b Program in Biophysics, Department of Chemistry, University of Michigan, Ann Arbor, MI, 48109-1055, USA*
*c Munich Center for Integrated Protein Science (CIPS-M) at Department of Chemistry, Technische Universität München, 85747 Garching, Germany*
*d Helmholtz Zentrum München, Institut of Structural Biology (STB), Ingolstädter Landstr. 1, 85764 Neuherberg, Germany*
*e Helmholtz Zentrum München, Institut of Developmental Genetics (IDG), Ingolstädter Landstr. 1, 85764 Neuherberg, Germany*
*f Helmholtz Zentrum München, Institute of Experimental Genetics (IEG), Ingolstädter Landstr. 1, 85764 Neuherberg, Germany*
*g German Center for Diabetes Research (DZD e.V.), 85764 Neuherberg, Germany*
*h Departament of Chemistry, Universidad Nacional de Colombia, Carrera 30 # 45-03 (Ciudad Universitaria), 111321 Bogota, Colombia*
*i Helmholtz Zentrum München, Research Unit Analytical Pathology (AAP), Ingolstädter Landstr. 1, 85764 Neuherberg, Germany*
*j Central European Institute of Technology (CEITEC), Masaryk University, Kamenice 5, 62500 Brno, Czech Republic*

## Materials and Methods

### Recombinant hIAPP expression and purification

Human IAPP was expressed and purified as described previously [1]. The peptide is fully oxidized amidated at the C-terminus. For all experiments, peptide poweder was dissolved into the buffer or plasma samples. Molecular biology reagents were obtained from Roche, Sigma-Aldrich St. Louis, MO, USA and New England Biolabs. Isotopically labeled nutrients were acquired from Cambridge Isotope Laboratories (CIL).

### Animal studies

To study the interaction between hIAPP and plasma, human islet amyloid polypeptide transgenic mice (TG/TG, +/TG) as well as and healthy controls (+/+) were employed [2]. EDTA plasma was collected as published previously [3, 4].

### Cell toxicity assay

To quantify cellular toxicity, cells of the pancreatic beta-cell line b-tc3 (obtained from Thermo Fisher Scientific) were plated into 96-well culture plates (1.500 cells/well), using Dulbecco's modified Eagle's medium supplemented with 10 % fetal bovine serum. After one day, cells were treated with sterile filtered compounds (hIAPP, LDL, glucose, fructose) in increasing concentration. The final volume of each well amounted to 100 µL. As 0 % and 100 % viability controls, 3 “no cell” and 3 “no compound” wells were included. Cells were incubated for 24 h at 37 °C, using a $CO_2$ incubator. Cell viability was measured using AquaBluer (MultiTarget Pharmaceuticals, LLC). For these experiments, the media in each well was replaced with the 100x diluted AquaBluer medium. The plates were subsequently returned for 4 h to the $CO_2$ incubator. Thereafter, the fluorescence intensity was measured (excitation: 540nm, emission: 590 nm). The method is based on NADH/NADPH oxidase activity as an indicator of cell viability. The average fluorescence value (RFU) of the no-cell control (background) was subtracted from all other RFU values. The test RFU values were converted to % viability using the formula:

% viability = (RFUtest / RFU of the no-compound wells) x 100

### Hemolytic activity

Human erythrocytes (donated by a healthy 31-year-old female) were used to explore the hemolytic activity of the peptide. The blood was centrifuged and washed four times with a 0.9 % NaCl solution to dispose the plasma. hIAPP was dissolved in PBS buffer (pH 7.4), and added to the erythrocytes. Suspensions were incubated for 3 h at 37 °C. Samples were centrifuged, and the optical density of the supernatant was measured at 451 nm to determine the extent of hemolysis. Hypotonically lyzed erythrocytes were used as a standard for 100 % hemolysis. The experiment was repeated three times including positive and negative controls.

### Western blot analysis

Purified hIAPP was dissolved into 30 µL of a 30 mM acetic acid solution (pH 5.3) and vortexed. Subsequently, 470 µL of plasma and 10 µL of SDS sample buffer were added. Glucose, fructose and LDL were prepared as concentrated stock solution and added directly to the peptide solution to yield the desired final concentrations. Samples were boiled for 5 min at 90 °C and separated by 12 % protein gels. The resolving gel was composed of: 3.3 mL dH2O, 4 mL 30% acrylamide mix (Roth Cat.Nr.: 3029.1), 2.5 mL 1.5 M Tris (pH : 8.8), 100 µL 10 % SDS, 100 µL 10 % ammonuim persulphate, 4 µL TEMED (Roth Cat.Nr.: 2367.3); The staking gel consisted of: 1.4 mL $dH_2O$, 330 µL 30 % acrylamide mix (Roth Cat.Nr.: 3029.1), 250 µL 1M Tris (pH 6.8), 20 µL 10% SDS, 20 µL 10% ammonium persulphate, 2 µL TEMED. The final running gel was transferred onto a Tnas-Blot-TurboTM Mini PVDF membrane with a Bio-Rad Trans-Blot TurboTM transfer system. The membrane was blocked in nonfat dry milk (Roth) with Tween-Tris-buffered saline with 5 % (w/v) for 1 hour and then incubated with the primary antibody A133 [5] in Tween-Tris-buffered saline with

a ratio 1:1000 overnight at 4 °C. Immunoreactivity was analyzed with an antirabbit peroxidase-conjugated secondary antibody (Serva) and chemiluminescence detection (Bio-Rad).

**Protein-lipid overlay assay**

Membrane Lipid Strips™ from Echelon (Cat.Nr.: P-6002) have been spotted with 100 pmol of fifteen different biologically important lipids. Membrane lipid strips were initially blocked with 5 mL of blocking buffer (PBS-T, 0.1 % v/v Tween-20; 3 % BSA free fat) and gently agitated for one hour at room temperature (RT). The blocking buffer was discarded. 2.5 nM of protein was dissolved in 5 mL PBS-T 3%. The membrane was incubated for 1 hr at RT with gentle agitation. Strips were washed three times with 5 mL PBS-T under gentle agitation for 5-10 min. Next, the primary antibody A133 [5] was added to 3 mL of a PBS-T 3% BSA blocking solution at a ratio 1:1000. The membrane was incubated for 1 h at RT with gentle agitation. The washing protocol was repeated and the membrane was finally incubated with the antirabbit peroxidase-conjugated secondary antibody (Serva) at a ratio of 1:5000 into PBS-T 3% BSA blocking solution followed by incubation at RT for 1 h. The membrane was finally washed again and blotted as in the WB experiments.

**NMR experiments**

All NMR experiments were performed using Bruker Avance 500, 600, 850 MHz spectrometers, equipped with cryo-probes. The $^{15}N$ and $^{13}C$ shifts were referenced indirectly. The proton chemical shift was referenced relative to the water resonance frequency. Backbone assignments were obtained via triple resonance experiments [6] employing a perdeuterated sample. The backbone chemical shifts (Cα, N, NH) were used to calculate the Random Coil Index (RCI), using webserver from the Wishart lab [7]. For the NMR data were processed using the software TopSpin (Bruker). Spectra were analyzed using ccpNMR analysis [8].

**Transmission electron microscopy (TEM)**

To prepare samples for TEM, 10 µL of each sample was placed on the EM grid for 1 min, followed by a drying procedure with filter paper. The grid was subsequently washed three times by adding a drop of water for 3 s, and drying it each time with filter paper. For staining, 10 µL of a 1% uranyl acetate solution was added for 30 s. The excess of the solution was dried with filter paper. Grids were purchased from Electron Microscopy Sciences (Hatfield, PA 19440, USA; Formvar/Carbon 300 mesh copper coated). Samples were measured immediately employing an EM 10 CR (Zeiss, Germany).

**Fluorescence experiments**

The fluorescence experiments were performed using a spectrofluorimeter PTI QuantaMaster™ 40, using Quartz cells with a path length of 5 nm. Samples were freshly prepared and transferred directly into the cell while stirring at RT. Experiments were carried out using a constant excitation wave length of 305 nm. The emission was scanned in the range between 200 to 600 nm. Solutions were prepared by adding NMR buffer (30 mM d-acetic acid, pH 5.3) to the dried peptide immediately prior to the measurements, keeping the solution on ice at all the times. The final hIAPP concentration amounted to 40 µM. The data were analyzed using the software Origin (OriginLab Corporation, Northampton, MA 01060, USA).

**Light microscopy**

DIC and fluorescence images were acquired using a Leica DMi8 CS Bino widefield fluorescence microscope using GFP and DAPI filter sets or DIC optics and recorded with a cooled charge-coupled device camera. A Leica oil immersion 100x objective was used with an ND of 1.49.

In the fluorescence images, the green and blue fluorescence was detected using a GFP filter (excitation at 450 nm - 490 nm; emission at 500 nm - 550 nm) and a DAPI filter (excitation at 325 nm - 375 nm; emission at 435 nm - 485 nm), respectively.

**Thioflavin-T assay**

To monitor the aggregation kinetics of hIAPP in presence and absence of LDL, fructose and glucose, we performed Thioflavin-T (ThT) assays. The peptide was dissolved in NMR buffer (30 mM d-acetic acid, pH 5.3) at a maximum concentration of 150 μM and maintained on ice at all times. For the experiments, this stock solution was diluted into the appropriate buffers (10 μM ThT; 20 mM $PO_4$, pH 7.4, or 30 mM acetate, pH 5.3) to a final peptide concentration of 10 μM. To test the influence of cosolvents that are enriched in the plasma of diabetic patients, buffers contained 2 μM LDL, 35 mM glucose or fructose. Samples were subsequently plated in triplicate on uncoated Fisherbrand 96-well polystyrene plates. Readings were taken on a Biotek Synergy two microplate reader. Samples were incubated at 25 °C for 24 h in the instrument with continuous, slow orbital shaking. Wells were read from the bottom with an excitation wavelength of 440 nm (30 nm bandwidth) and an emission wavelength of 485 nm (20 nm bandwidth) at 3-min intervals. Following data acquisition, the raw fluorescence traces were background corrected and normalized. Normalized curves were subsequently plotted using the software Origin (OriginLab Corporation, Northampton, MA 01060, USA).

**Competing financial interests**.

The authors declare no competing financial interests.

**Author Contributions**

D.C.R.C., B.R., D.G., and A.R.C. designed the experiments. D.C.R.C. expressed, purified and characterized hIAPP. D.C.R.C., K.T., R.S., F.S., and G.G. performed NMR experiments and analyzed the data. A.F, M.S., and M.H.d.A. extracted and processed the mouse plasma samples. M.H., S.C., A.R.C. and C.A.S. performed the fluorescence and ThT experiments and analysis. S.S. performed the DLS experiments. D.C.R.C., Y.M. and M.F. contributed the DIC microscopy experiments and analysis. D.C.R.C., K.B. and M.C. performed the western blot analysis, lipid blot assay and cell toxicity. D.C.R.C. performed the hemolytic activity assay. D.C.R.C., M.A., G.M. and A.K.W. carried out EM experiments and analysis. D.C.R.C., D.G, F.S., A.F., A.R. and B.R. wrote the manuscript with contributions from all authors.

**Conflicts of interest**

The authors declare no conflicts of interest.

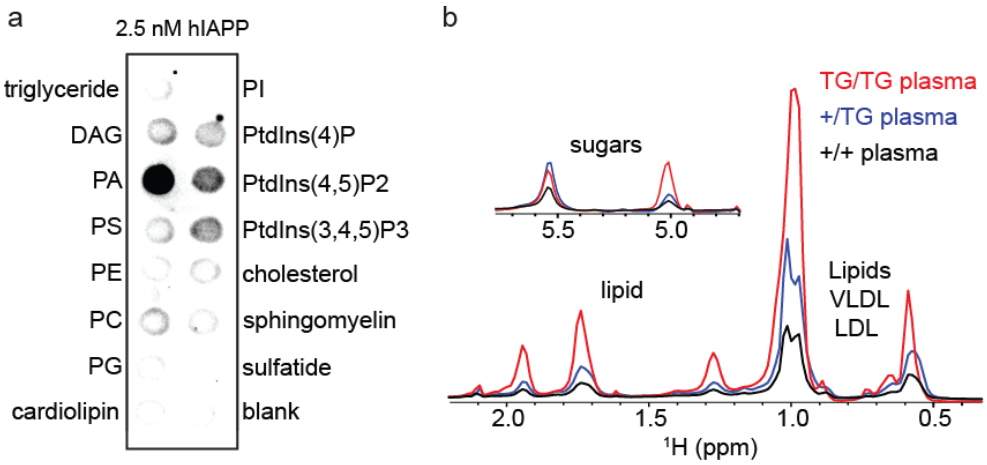


***Figure S1***. *a) Lipid strip blot assay performed with a 2.5 nM hIAPP sample. hIAPP was identified using the hIAPP specific antibody A133* [5]*. We find that hIAPP interacts weakly with triglycerides, cholesterol, phospholipids, while a stronger interaction is observed for phosphatidylglycerides and in particular with phosphatidic acid. b) Comparison of the* $^{1}$*H- NMR spectra of hIAPP in the plasma of TG/TG (red), +/TG (blue) and +/+ mice (black) with assignments of the major plasma components. In agreement with previous resuls, we find that the amount of lipids (VLDL and LDL) as well as lactate, valine, and sugars is strongly increased in the TG/TG plasma* [9]*.*

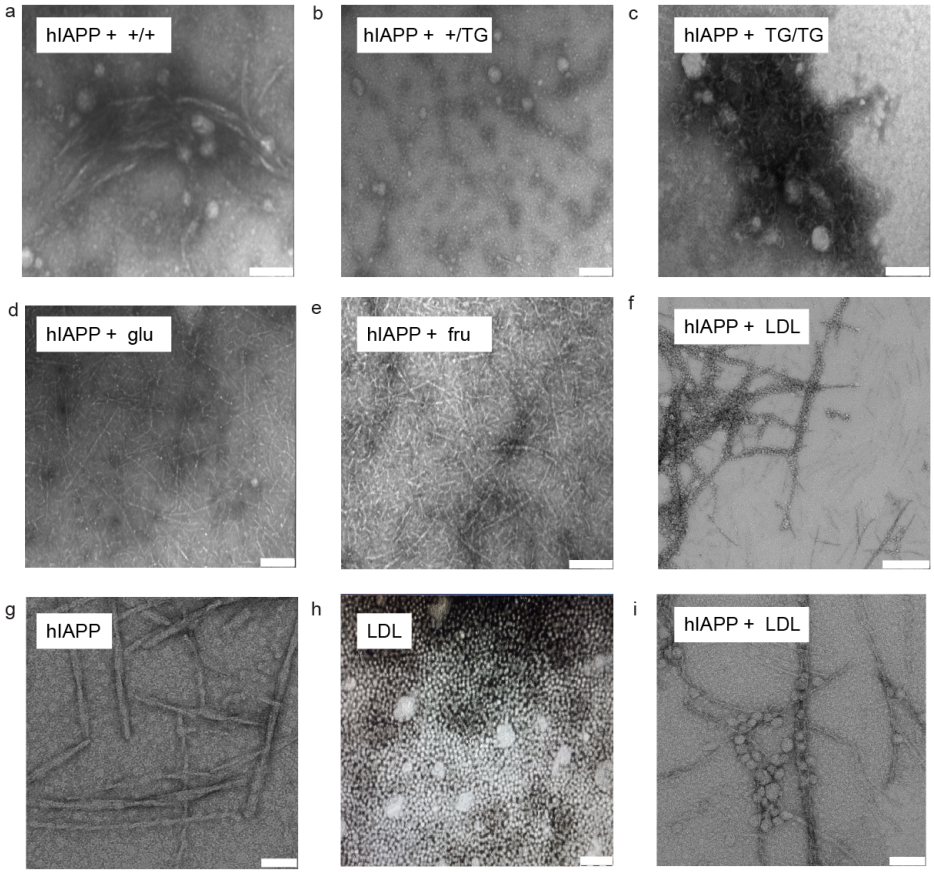


***Figure S2***. ***Transmission electron microscopy (EM) shows that the hIAPP aggregation state is affected by plasma, LDL, glucose and fructose.*** *hIAPP in the presence of* ***a*** *+/+ blood plasma,* ***b*** *+/TG plasma,* ***c*** *TG/TG plasma,* ***d*** *35 mM glucose,* ***e*** *35 mM fructose,* ***f*** *2 µM LDL.* ***g*** *hIAPP fibrils control (100 µM, pH 7.5).* ***h*** *2 µM LDL control.* ***i*** *hIAPP in presence of 2 µM LDL (different region of the grid). EM images have been recorded after completion of the NMR experiments shown in Figure 1. Scale bars represent a length of 200 nm.*

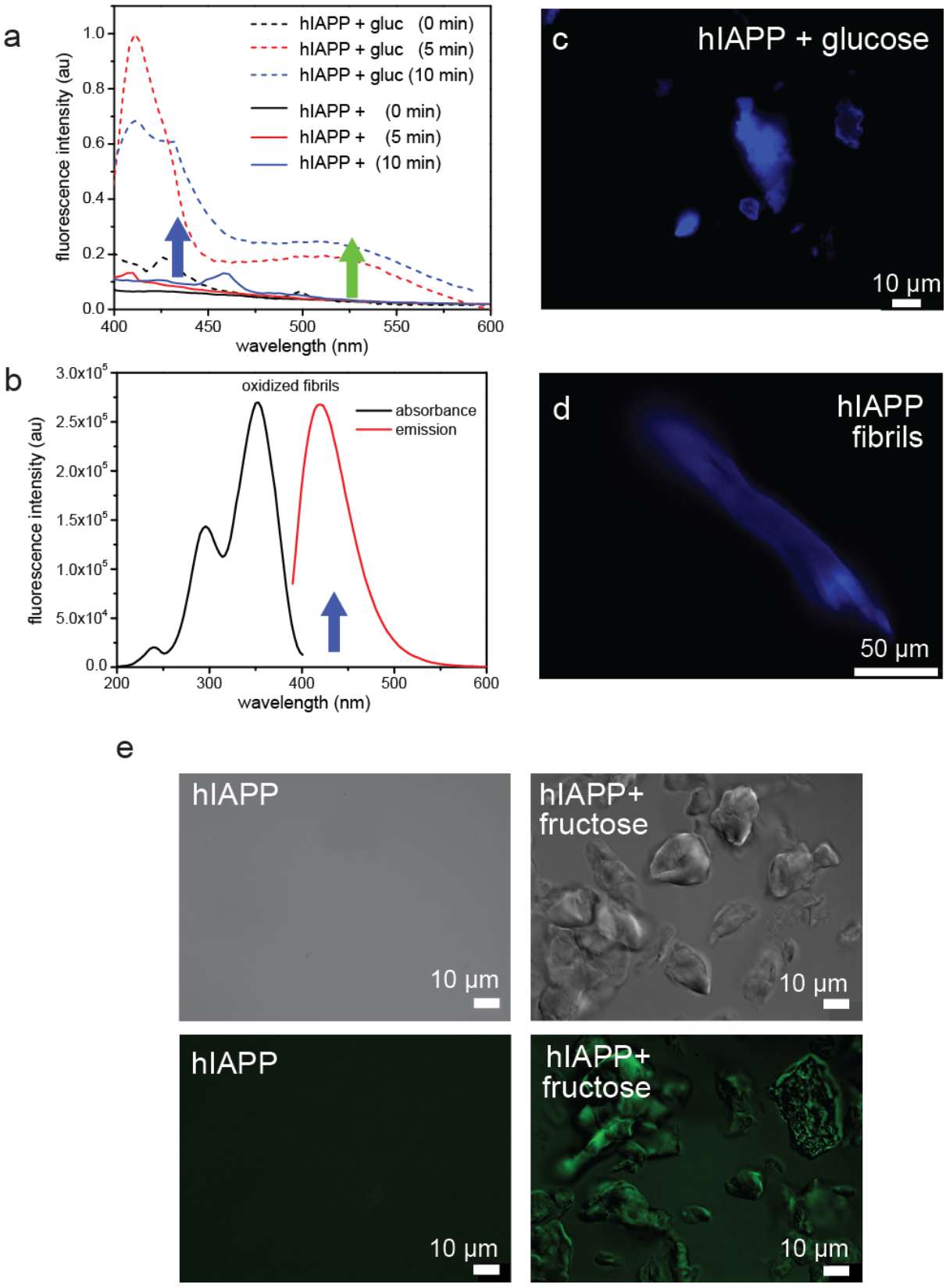


***Figure S3**. **Intrinsic fluorescence of glucose and LDL induced hIAPP oligomeric assemblies. a** Fluorescence emission spectra of a 40 µM hIAPP solution in the presence and absence of 35 mM glucose monitored over the time (excitation at 305 nm, emission at 400-600 nm). The emission signal is increasing in the presence of glucose as a function of time, suggesting that the interaction between hIAPP and sugars is very dynamic. The solutions were prepared using NMR buffer (30 mM d-acetic*

*acid, pH 5.3). The blue and green arrow indicate emission signal passing through the GFP and DAPI filter, respectively.* ***b*** *Absorbance (black) and emission (red, with excitation at 305 nm) spectra of preformed oxidized hIAPP fibrils (in 30 mM d-acetic acid, pH 5.3).* ***c*** *Fluorescence image of a freshly dissolved solution containing 40 μM hIAPP and 35 mM glucose, using a DAPI filter.* ***d*** *Fluorescence image of preformed oxidized hIAPP fibrils using a DAPI filter (excitation at 325 nm - 375 nm; emission at 435 nm - 485 nm). We propose that sugars capture the peptide in a colloidal like state, in which the hIAPP retains a high degree of flexibility, but is structured enough to yield intrinsic fluorescence which is presumably due to the an extension of the conjugation of the peptide bond.* ***e*** *DIC and GFP-filtered fluorescence microscopy images of hIAPP in the absence and presence of fructose.*

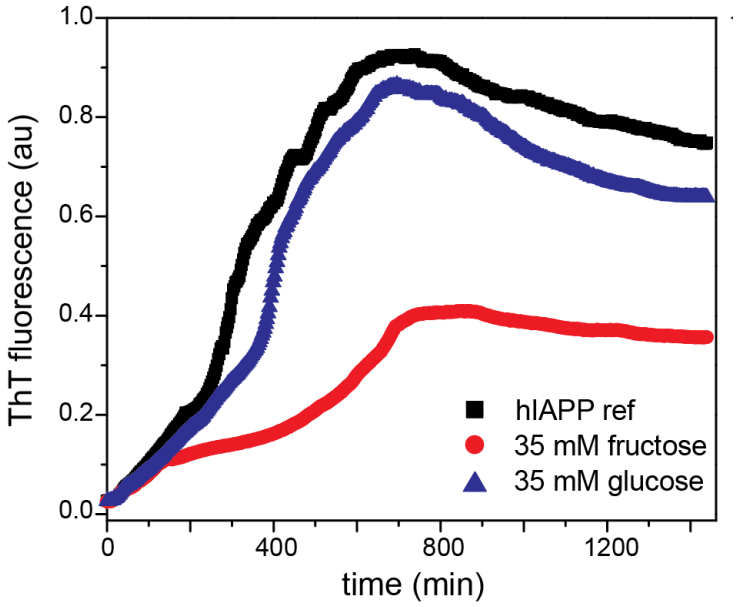


***Figure S4****. Thioflavin T (ThT) aggregation kinetics after incubation of hIAPP with 35 mM glucose (blue) and 35 mM fructose (red). The strongest effect on inhibiton of aggregation is seen in the presence of fructose.*

## References


1. D. C. Rodriguez Camargo, K. Tripsianes, T. G. Kapp, J. Mendes, J. Schubert, B. Cordes and B. Reif, *Protein Expr. Purif.*, 2015, **106**, 49–56.
2. A. Franko, D. C. Rodriguez Camargo, A. Böddrich, D. Garg, A. Rodriguez Camargo, J. Rozman, B. Rathkolb, D. Janik, M. Aichler, A. Feuchtinger, F. Neff, H. Fuchs, E. E. Wanker, B. Reif, H.-U. Häring, A. Peter and M. Hrabě de Angelis, *Sci. Rep.*, 2018, **8**, article no. 1116.
3. A. Franko, P. Huypens, S. Neschen, M. Irmler, J. Rozman, B. Rathkolb, F. Neff, C. Prehn, G. Dubois, M. Baumann, R. Massinger, D. Gradinger, G. K. H. Przemeck, B. Repp, M. Aichler, A. Feuchtinger, P. Schommers, O. Stöhr, C. Sanchez-Lasheras, J. Adamski, A. Peter, H. Prokisch, J. Beckers, A. K. Walch, H. Fuchs, E. Wolf, M. Schubert, R. J. Wiesner and M. H. de Angelis, *Diabetes*, 2016, **65**, 2540-2552.
4. A. Franko, S. Neschen, J. Rozman, B. Rathkolb, M. Aichler, A. Feuchtinger, L. Brachthauser, F. Neff, M. Kovarova, E. Wolf, H. Fuchs, H. U. Haring, A. Peter and M. H. de Angelis, *Mol. Metabol.*, 2017, **6**, 256-266.
5. J. F. Paulsson and G. T. Westermark, *Diabetes*, 2005, **54**, 2117-2125.
6. M. Sattler, J. Schleucher and C. Griesinger, *Prog. NMR Spect.*, 1999, **34**, 93-158.
7. M. V. Berjanskii and D. S. Wishart, *J. Am. Chem. Soc.*, 2005, **127**, 14970-14971.
8. W. F. Vranken, W. Boucher, T. J. Stevens, R. F. A. Pajon, M. Llinas, E. L. Ulrich, J. L. Markley, J. Ionides and E. D. Laue, *Proteins*, 2005, **59**, 687-696.
9. W. Yabsley, S. Homer-Vanniasinkam and J. Fisher, *ISRN Vasc. Med.*, 2012, **2012**.